Unveiling membrane thermoregulation strategies in marine picocyanobacteria

Solène Breton, Juliette Jouhet, Ulysse Guyet, Valérie Gros, Justine Pittera, David Demory, Frédéric Partensky, Hugo Doré, Morgane Ratin, Eric Maréchal, et al.

DR CHRISTOPHE SIX (Orcid ID : 0000-0002-8506-1149)

Article type : Regular Manuscript

Unveiling membrane thermoregulation strategies in marine picocyanobacteria

Solène Breton[1], Juliette Jouhet[2], Ulysse Guyet[1], Valérie Gros[2], Justine Pittera[1], David Demory[3], Frédéric Partensky[1], Hugo Doré[1], Morgane Ratin[1], Eric Maréchal[2], Ngoc An Nguyen[1], Laurence Garczarek[1] & Christophe Six[1]

[1] Sorbonne Université, Centre National de la Recherche Scientifique, UMR 7144 Adaptation et Diversité en Milieu Marin (AD2M), Ecology of Marine Plankton (ECOMAP) Team, Station Biologique de Roscoff (SBR), 29680 Roscoff, France.

[2] Laboratoire de Physiologie Cellulaire et Végétale, Unité mixe de recherche 5168 CNRS, CEA, INRA, Université Grenoble Alpes, IRIG, CEA Grenoble, 17, rue des Martyrs, 38000 Grenoble, France.

[3] School of Biology, Georgia Institute of Technology, Atlanta, GA 30332, USA.

To whom correspondence should be addressed: Christophe Six, email: christophe.six@sb-roscoff.fr, Phone: +33 2 98292534

Received: *8 July 2019*

Accepted: *29 September 2019*

This article has been accepted for publication and undergone full peer review but has not been through the copyediting, typesetting, pagination and proofreading process, which may lead to differences between this version and the Version of Record. Please cite this article as doi: 10.1111/NPH.16239

ORCID information:

Christophe Six: https://orcid.org/0000-0002-8506-1149

Juliette Jouhet : https://orcid.org/0000-0002-4402-2194

Laurence Graczarek : https://orcid.org/0000-0002-8191-8395

Frédéric Partensky: https://orcid.org/0000-0003-1274-4050

Eric Maréchal: https://orcid.org/0000-0002-0060-1696

Valérie Gros: https://orcid.org/0000-0002-6082-4613

David Demory: https://orcid.org/0000-0003-4928-8925

Hugo Doré: https://orcid.org/0000-0003-4160-3679

Summary

. The wide latitudinal distribution of marine *Synechococcus* cyanobacteria partly relies on the differentiation of lineages adapted to distinct thermal environments. Membranes are highly thermosensitive cell components and the ability to modulate their fluidity can be critical for the fitness of an ecotype in a particular thermal niche.

. We compared the thermophysiology of *Synechococcus* strains representative of major temperature ecotypes in the field. We measured growth, photosynthetic capacities and membrane lipidome variations. We carried out a metagenomic analysis of stations of the *Tara* Oceans expedition to describe the latitudinal distribution of the lipid desaturase genes in the oceans.

. All strains maintained efficient photosynthetic capacities over their different temperature growth ranges. Subpolar and cold temperate strains showed enhanced capacities of lipid monodesaturation at low temperature thanks to an additional, poorly regiospecific Δ9-desaturase. In contrast, tropical and warm temperate strains displayed moderate monodesaturation capacities but high proportions of double unsaturations in response to cold, thanks to regiospecific Δ12-desaturases. The desaturase genes displayed specific distributions directly related to latitudinal variations in ocean surface temperature.

. This study highlights the critical importance of membrane fluidity modulation by desaturases in the adaptive strategies of *Synechococcus* cyanobacteria during the colonization of novel thermal niches.

Key words: cyanobacteria, marine *Synechococcus*, membrane lipids, temperature ecotype, adaptation

Introduction

Marine *Synechococcus* are among the smallest photoautotrophs on Earth but are thought to be responsible for about 17% of the global marine net primary production (Flombaum *et al.*, 2013). They constitute a much diversified cyanobacterial radiation, most of them being gathered in the phylogenetic subcluster 5.1 *sensu* Herdman *et al.* (2001) that, according to analyses based on the *petB* gene marker, includes 15 clades and 28 subclades (Mazard *et al.*, 2012). A number of phylogeographic studies have shown that five clades (I, II, III, IV and CRD1) predominate in the ocean, occupying different environmental niches. Clades I and IV co-occur in nutrient-rich, temperate and cold regions, whereas clades II and III are usually found in warmer waters, with clades II et III dominating in N and P-depleted areas, respectively (Zwirglmaier *et al.*, 2008; Sohm *et al.*, 2015; Farrant *et al.*, 2016; Paulsen *et al.*, 2016; Kent *et al.*, 2018). More recently discovered, the fifth major clade, CRD1, appears to be specialized to iron-limited environments, such as the so-called High Chlorophyll Low Nutrients areas of the South Pacific Ocean (Sohm *et al.*, 2015; Farrant *et al.*, 2016; Kent *et al.*, 2018).

The wide latitudinal distribution of marine *Synechococcus*, spanning from the equator to polar circles (Zwirglmaier *et al.*, 2008; Huang *et al.*, 2012), suggests that the different lineages have developed efficient strategies to colonize distinct thermal environments. Several studies have shown that representative strains of specific clades exhibit thermal *preferenda* that are in good agreement with the temperature of their isolation sites (Pittera *et al.* 2014; Mackey *et al.* 2013; Varkey *et al.* 2016; Moore *et al.* 1995). These genetically distinct lineages, physiologically adapted to distinct niches, thus constitute 'temperature ecotypes', a.k.a. 'thermotypes', a concept previously defined for the other dominant marine cyanobacterium *Prochlorococcus* (Johnson *et al.*, 2006; Coleman & Chisholm, 2007). The physiological bases that underpin the process of thermal niche partitioning of marine picocyanobacteria remain, however, poorly known. Several studies suggest that the ability to adapt the photosynthetic mechanisms to different temperatures could constitute a bottleneck for the competitiveness in different thermal environments (Pittera *et al.*, 2014, 2016). In particular, it has been shown that the photosystem II of different *Synechococcus* temperature ecotypes is differentially affected by thermal stress (Pittera *et al.*, 2014), and that their photosynthetic antenna, called the phycobilisome, display

differential functional stability consistent with the temperature *preferenda* of the strains (Pittera *et al.*, 2016). Another important component that may directly impact the smooth running of the photosynthetic apparatus at different temperatures is the lipid matrix of thylakoid membranes. It is indeed well known that membranes are among the most thermosensitive cell components, because temperature drastically affects their fluidity and permeability and therefore the activity of all the membrane-embedded proteins (Mikami & Murata, 2003). The ability to modulate the fluidity of membranes, notably the thylakoids, can thus be critical for the fitness of photosynthetic organisms in specific thermal niches.

Cyanobacterial membranes are composed of three main glycolipids, mono- and digalactosyldiacylglycerol (MGDG and DGDG) and a charged sulfolipid, sulfoquinivosyldiacylglycerol (SQDG). In addition, smaller amounts of a phospholipid, phosphatidyldiacylglycerol (PG) are usually observed (Murata & Wada, 1995). Whereas a number of studies have dealt with the membrane thermoregulation of freshwater cyanobacteria, the composition of the membranes and the impact of temperature in their marine counterparts remain poorly studied (Merritt *et al.*, 1991; Van Mooy *et al.*, 2009; Varkey *et al.*, 2016). A recent study has shown that the model marine strain *Synechococcus* sp. WH7803 contains membrane lipids with shorter fatty acid chains than freshwater cyanobacteria and is able to adjust its membrane fluidity to different growth temperatures (Pittera *et al.,* 2018). Indeed, in response to cold, the WH7803 strain induces the shortening of the fatty acid chains at the *sn*-1 position of the galactolipids, leading to membrane thinning, and activates fatty acid desaturation at specific sites of the three glycolipids (Pittera *et al.,* 2018).

Unsaturations can be dynamically inserted in fatty acid chains by lipid desaturase enzymes. The catalytic site of these enzymes comprises histidine-rich boxes, including a non-heme iron center whose activity requires electrons and oxygen (Los & Murata, 1998). Genomic studies of the fatty acid desaturase gene content in marine *Synechococcus* have shown the presence of four main distinct genes in the genomes, encoding two Δ9- (*desC3* and *desC4*) and two Δ12-desaturases (*desA2* and *desA3*; Chi *et al.*, 2008; Varkey *et al.*, 2016). A closer look at the phyletic profiles of these four genes unveiled that the marine *Synechococcus* strains representative of the four dominant clades (I through IV) exhibit distinct desaturase gene contents, suggesting that the

desaturation capacities could be part of the physiological strategies underlying the specialization of these lineages to different thermal environments (Pittera *et al.,* 2018). However, it is not yet known how these differential gene contents affect the composition and thermoacclimation processes of the membrane lipidome in the different temperature ecotypes.

In this study, we analyzed the composition of the membrane lipidome of a selection of four strains representative of each of the four dominant marine *Synechococcus* clades (I-IV) in natural communities and we unveiled marked differences in the respective regulation processes adjusting membrane fluidity in response to temperature. Furthermore, we show that the global oceanic distribution of the desaturase genes is fully consistent with their differential distribution among the ecotypes, demonstrating the significance of these thermoadaptation strategies in thermal niche partitioning of *Synechococcus in situ*. We discuss these findings in the context of the important role of marine *Synechococcus* in the ocean primary productivity.

Materials and methods

Growth conditions and experimental design

Four marine *Synechococcus* strains retrieved from the Roscoff Culture Collection (http://roscoff-culture-collection.org/) were used in this study (Table 1): MVIR-18-1 (clade I), A15-62 (clade II), WH8102 (clade III) and BL107 (clade IV), of which only WH8102 was axenic. Strains were grown in PCR-S11 culture medium (Rippka *et al.*, 2000; Moore *et al.*, 2007) supplemented with 1 mM sodium nitrate under low irradiance (20 µmol photons m^{-2} s^{-1}), in order to ensure the presence of several thylakoidal lamellae in the cells (Kana & Glibert, 1987). Continuous light was provided by multicolor LED systems (Alpheus, France). The axenicity of *Synechococcus* sp. WH8102 cultures and minimal contamination levels of the other strains (<20%) was regularly checked by flow cytometry using SYBR-Green staining (Marie *et al.*, 2001).

Cultures of the four cyanobacteria were acclimated for several weeks to a range of temperatures (10 to 30°C) in temperature-controlled chambers (Lovibond, Germany), monitored by flow cytometry and sampled during the exponential growth phase to measure photosynthetic parameters and analyze the membrane lipid structure in acclimated state. To study the dynamics

of the temperature-induced remodeling of the membranes, we also carried out temperature shift experiments. Three liters of exponentially growing cultures (at 1-3 10^7 cell mL^{-1}) maintained at 22°C were split into subcultures and transferred to either 13°C or 30°C, under identical light conditions. One subculture per condition was harvested every day during four days. All experiments were repeated three to four times.

Flow cytometry, in vivo *fluorimetry and pigment analyses*

Aliquots of cultures were preserved using 0.25% (v/v) glutaraldehyde final concentration (grade II, Sigma Aldrich, St Louis, MO, USA) and stored at -80°C until analysis. Cell concentrations were determined using a flow cytometer (FACS Canto II, Becton Dickinson, San Jose, CA, USA) as described previously (Pittera *et al.*, 2014). Growth rates were calculated on cultures pre-acclimated to a range of temperatures as the slope of a ln*(Nt) vs.* time plot function, where *Nt* is the cell concentration at time t. The growth models of Bernard and Rémond (2012) and Boatman *et al.* (2017) were used to model the optimal temperature for growth (T_{OPT}) and the temperature limits for growth (T_{MIN} and T_{MAX}; for more details, see Notes S1).

The photosystem II quantum yield (F_V/F_M) was measured using a Pulse Amplitude Modulation fluorometer (PhytoPAM I, Walz Effeltrich, Germany) in the presence of 100 µM of the PSII blocker 3-(3,4-dichlorophenyl)-1,1-dimethylurea (DCMU), following a previously described procedure (Pittera *et al.*, 2014). The quantum yield was calculated as:

$$F_V/F_M = (F_M-F_0)/F_M$$

where F_0 is the basal fluorescence level, F_M the maximal fluorescence level and F_V the variable fluorescence (Campbell *et al.*, 1998; Ogawa *et al.*, 2017).

For pigment analyses, 50 to 100 mL of culture were harvested by centrifugation during 10 min, at 4°C and 20,000 x *g* (Eppendorf 5804R) in the presence of 0.01% (v/v) pluronic acid (Sigma Aldrich, St Louis, MO, USA). The cell pellets were covered with 200 µL of cold methanol (HPLC Grade, Sigma Aldrich, St Louis, MO, USA), vortexed until complete resuspension and incubated for 30 min on ice. The pigment extracts were vortexed again and then centrifuged as described above (Eppendorf 5417R). The supernatants were transferred and supplemented with 10% (v/v) distilled water final volume, in order to avoid peak distortion. Pigments were measured by high

pressure liquid chromatography using an HPLC 1100 Series System equipped with a photodiode array (Hewlett-Packard, St Palo Alto, CA, USA) as previously described (Pittera *et al.*, 2014).

Membrane lipidome analyses

The global detailed procedure has been previously published in Jouhet *et al.*, 2017 and Pittera *et al.*, (2018). For each condition, 400 mL of culture were harvested by two successive centrifugation steps of 10 min, at 20,000 x *g* and 4°C (centrifuges Beckman Avanti J-25 and Eppendorf 5804R) and stored at -80°C until analysis. Membrane lipids were extracted in glass hardware following a modified version of the Bligh and Dyer (1959) procedure (Pittera *et al.* 2018).

Fatty acid regiolocalization - We first identified the positional distribution of the fatty acids esterified to the four main glycerolipids of the four *Synechococcus* strains samples. Each strain was grown at three different temperatures spanning their respective thermal growth range. The glycerolipids were then extracted and separated by 2-dimensional thin layer chromatography as previously described (Pittera *et al.*, 2018). Glycerolipids spots were revealed under UV light in the presence of malvidine-3-O-galactoside (primuline, 0.2% in pure methanol, Sigma Aldrich, St Louis, MO, USA) and scraped off the plate. Each separated lipid class were recovered from the silica by extraction in glass hardware and dried under nitrogen gas. The position of the different fatty acid molecular species esterified to the glycerol backbone of the purified glycerolipids was determined by MS/MS analyses as described in (Jouhet et al., 2017).

Lipid quantification - The quantity of fatty acids in the samples was first determined by gas chromatography coupled with a flame ionization detector (GC-FID). The lipid samples were first methanolyzed and analyzed following a previously described procedure (Jouhet *et al.*, 2017). The lipid samples were then prepared in order to inject 25 nmol of total fatty acids dissolved in 100 µL of chloroform/methanol [2/1, (v/v)] containing 125 pmol of each internal standard. The membrane lipids were separated by HPLC (Agilent 1200) equipped with a diol column (150 mm x 3 mm x 5 µm; Macherey-Nagel) at 40°C and quantified by MS/MS with a triple quadrupole mass spectrometer equipped with a jet stream electrospray ion source (Agilent 6460) (Jouhet *et al.*, 2017; Pittera *et al.*, 2018). Mass spectra were processed with the Agilent MassHunter Workstation software for lipid identification and quantification. Lipid amounts (pmol) were

corrected for response differences between internal standards and endogenous lipids and by comparison with a qualified control (QC). QC extract corresponded to a known lipid extract from *Arabidopsis* cell culture qualified and quantified by TLC and GC-FID as described in Jouhet *et al.* (2017).

In situ *metagenomic analyses*

***Tara* Oceans dataset** - We analyzed 33 metagenomes collected from surface waters during the *Tara* Oceans expedition (Sunagawa *et al.*, 2015; http://www.taraoceans-dataportal.org). Metagenomes corresponding to the bacterial size fraction (0.2-1.6 µm for TARA_004 to TARA_052 and 0.2-3 µm for the other stations) were sequenced as 100-108 bp Illumina overlapping paired-end reads. Reads were merged using FLASH v1.2.7 (Magoč & Salzberg, 2011) and trimmed with CLC QualityTrim v4.10.86742 (CLC Bio), resulting in 100-215 bp fragments. Temperature data for each station were retrieved from PANGAEA (https://doi.pangaea.de/10.1594/PANGAEA.840718).

Functional assignment of metagenomics data - Reads were first recruited against a database of 155 protein sequences of the four lipid desaturases (DesC3, DesC4, DesA2, DesA3) extracted from the 53 *Synechococcus*/*Cyanobium* genomes of the information system Cyanorak v2 (http://sb-roscoff.fr/Phyto/cyanorak; Pittera et al., 2018; Dataset S1) using BLASTX analyses (v 2.7.1+; Altschul *et al.*, 1990) with default parameters, limiting the results to one target sequence (--max_target_seqs 1), and considering only the results with an e-value lower than 0.001. The recruited reads were then mapped with BLASTN (with the same options as above) against a database including the 155 above mentioned *Synechococcus*/*Cyanobium* desaturases as well as many sequences used as outgroups including 117 *Prochlorococcus* fatty acid desaturase sequences (Dataset S2), 185 outgroup cyanobacterial genomes from Cyanobase plus 537 genomes from proGenomes (Dataset S3), 6,092 additional non-picocyanobacterial fatty acid desaturase sequences retrieved from NCBI (Dataset S4) as well as all marine picocyanobacterial desaturases from Cyanorak. Reads showing a best hit to outgroup sequences or with less than 90% of their sequence aligned were removed and the remaining reads were assigned to *Synechococcus* according to their BLASTN best hit. Reads were then functionally assigned to one

of the four desaturase clusters of likely orthologous genes (CLOGs) from the Cyanorak database based on their best hit sequence and read counts were normalized to the average gene length of each CLOG. In order to study the presence/absence of lipid desaturases with regard to thermal environments, only stations dominated by major Ecologically Significant Taxonomic Units (ESTU) of *Synechococcus* clades I to IV, namely ESTUs IA, IIA, IIIA or IVA-C *sensu* (Farrant *et al.*, 2016), were used. Furthermore, to ensure sufficient coverage for the results to be reliable, only stations with a minimum of 2,500 distinct CLOGs, corresponding to the average number of genes in *Synechococcus* genomes, were considered. Altogether 52% (33 out of 63) of the *Tara* Oceans stations have been retained for the analysis. Reads assigned to genes encoding the four lipid desaturases (*desC3*, *desC4*, *desA2*, *desA3*) were then extracted and their respective abundances were normalized to the corresponding *petB* reads abundance, retrieved from Farrant *et al.* (2016).

Results

Thermal preferenda *and photosynthetic activity*

We acclimated four *Synechococcus* strains isolated from different thermal environments to a global range of temperatures spanning from 10 to 32°C. The strains displayed thermal *preferenda* that significantly differed with regard to their thermal growth limits, especially at cold temperatures, and less so by their optimal growth temperature (Fig. 1A). The subpolar clade I strain MVIR-18-1 showed significant growth down to 9-10°C but could not cope with temperatures higher than 26°C. The cold-temperate clade IV strain BL107 grew between 14°C and 28°C, while the warm temperate clade III strain WH8102 and the tropical clade II strain A15-62 grew from 16°C to more than 32°C. Growth *vs.* temperature models were used to estimate the growth parameters (Table 1, Fig. S1). Although some differences in these parameters could be observed depending on the model used (Tables S1, S2), the subpolar and cold-temperate strains displayed lower estimates of T_{MIN} and T_{MAX} than the warm-adapted strains (see Notes S1).

The quantum yield of the photosystem II reaction center (F_V/F_M) remained generally high over the whole growth temperature ranges (Fig. 1B). The values were however somewhat lower

at cold growth temperatures (16°C) for strains WH8102 and A15-62, and at warm growth temperatures for the subpolar MVIR-18-1 and cold temperate BL107 strains.

The β-carotene to chl *a* ratio increased at high growth temperature and this trend was more pronounced for the warm temperature strains WH8102 and A15-62 (Fig. 1C). For all strains, the zeaxanthin to chl *a* mass ratio was high at low growth temperature and lower at high temperature. This ratio was globally higher in the subpolar strain MVIR-18-1 and in the temperate strain BL107 than in the two other strains (Fig. 1D). These variations probably mostly originated from an increase in the zeaxanthin cell content with decreasing temperature, as suggested by the cold-induced increase of the zeaxanthin to β-cryptoxanthin ratio, the direct precursor of zeaxanthin in its biosynthetic pathway (Fig. S2). It is also likely that the chl *a* cell content decreased in response to cold.

Membrane lipidomic analyses

General composition of the membrane lipidome – We analyzed the composition of the total membrane lipidome, which in cyanobacteria includes a very high proportion of the thylakoidal lipids. The 2-dimensional thin layer chromatography (TLC) analyses revealed four major spots corresponding to the lipid classes usually observed in cyanobacteria: MGDG, DGDG, SQDG and PG. In total, there were about 30 different molecular species of complex lipids in the four studied strains of marine *Synechococcus*. The two galactolipids (MGDG and DGDG) were generally the major components of membranes and the fatty acids bound to these lipids were mostly C14, C16 and traces of C18 fatty acid chains. The number of unsaturations on these chains never exceeded 2. The global composition of the fatty acids bound to the four different lipids in these strains, reported in detail in Tables S3-6 and on Figs. S3-6 (see Notes S2), was overall similar to *Synechococcus* sp. WH7803 (Pittera *et al.*, 2018). The *sn*-1 position most often bound C16 chains, whereas the *sn*-2 bound exclusively C14 chains on the galactolipids (Figs. S3-4) and a mix of C14 and C16 chains on SQDG (Fig. S5).

PG is present in heterotrophic bacteria, complicating the interpretation of the PG data of the 3 non-axenic strains. In cyanobacteria, this minor lipid is thought to play roles in the stabilization of photosystems (Itoh *et al.*, 2012; Mizusawa and Wada, 2012; Boudière *et al.*, 2014) rather than being directly involved in membrane thermoacclimation processes, as supported by the results

for the axenic strains WH8102 and WH7803 (Pittera *et al.*, 2018; Fig. S6). Hereafter we therefore compare the major mechanisms involved in thermoacclimation only for the three major membrane glycolipids only present in cyanobacteria.

Membrane thickness variations in response to temperature - As palmitic (C16:0) and myristic (C14:0) fatty acid chains were dominant in all glycolipids of all strains, we used the C14:C16 molar ratio as a proxy for assessing the variations of the membrane thickness. In the four strains, such variations may occur at the *sn*-1 position of the two most abundant lipids, MGDG and DGDG, as already observed in *Synechococcus* sp. WH7803 (Pittera *et al.*, 2018), and at the *sn*-2 position of SQDG. The results showed an increase of the C14:16 ratio at the *sn*-1 position of MGDG and DGDG ratio in response to low growth temperatures only for the subpolar strain MVIR-18-1 and the tropical strain A15-62 (Fig. 2). This process was more pronounced for the MGDG than for to the DGDG. In contrast, BL107 and WH8102 strains showed a slight increase of the fatty acid length at these positions in response to low growth temperature. MVIR-18-1 was additionally capable of decreasing the length of the fatty acid bound to the *sn*-2 position of the SQDG in response to growth temperature lower than 14°C (Fig. S5). In the cultures grown at 22°C and shifted to either 13 or 30°C, only little variations of the C14:C16 ratio were observed (Figs. S7-14).

Mono-desaturation processes on galactolipids - MGDG showed the highest mono-unsaturation levels, with high proportions of 14:1 and 16:1 fatty acid chains. At the *sn*-1 position, the proportion of C16:1 chains increased in response to low growth temperature, especially in the subpolar strain MVIR-18-1 and the cold temperate strain BL107 (Fig. 3A-B). In contrast, the warm-adapted strains WH8102 and A15-62 showed much lower variations of the C16:1 relative level.

The proportion of C14:1 chains at the MGDG *sn*-1 position also increased at lower temperatures in all strains except for the warm temperate WH8102, for which the C14 species were low at this position. The largest C14:1 to C14:0 amplitude changes were achieved by the subpolar strain MVIR-18-1. It is likely that this resulted from the replacement of C16 chains by C14:1 chains in *de novo* synthetized MGDG molecules, rather than active desaturation of C14:0 chains by desaturase enzymes, inducing the abovementioned chain shortening. This conclusion is

supported by the fact that no rapid complementary decrease of C14:0 was observed in acclimated cultures (Fig. 3) nor during thermal shift experiments (Fig S7, S11).

The proportion of C14:1 chains increased at the MGDG *sn*-2 position in the subpolar MVIR-18-1 and in both temperate strains in response to low temperature, with WH8102 showing the largest changes (Fig.4A). Complementary changes between C14:0 and C14:1 chains were observed during the shift experiments, suggesting a Δ9-desaturation activity at this position (Fig. S7 and S11).

The DGDG showed overall similar variations to MGDG at both sn-1 (Fig. 3C, D) and sn-2 (Fig. 4B) positions, but the global C16 and C14 mono-unsaturation levels were however lower than for MGDG. This suggests the occurrence of an active C16:0 mono-desaturation process at the *sn*-1 site, especially for the subpolar strain MVIR-18-1, as also observed in the cold (Fig. S8) and warm (Fig. S12) shift experiment results. The insertion of *de novo* synthetized C14:1 chains at the DGDG *sn*-1 (Fig. 3D) and *sn*-2 (Fig. 4B) positions in cultures acclimated to low temperature were observable for all strains, but were weaker than for MGDG.

Mono-desaturation processes on SQDG - As already observed in *Synechococcus* sp. WH7803, SQDG showed a quite different fatty acid composition from the two galactolipids (Pittera *et al.*, 2018). In the four strains, the *sn*-1 position bound quasi exclusively C16 chains (Fig. S5) and was seemingly the site of an active Δ9-mono-desaturation activity in cultures acclimated to low temperature (Fig. 3E, F), as well as in cultures subjected to temperature shifts (Fig. S9, S13). The *sn*-2 position bound C14 and C16 chains, often in comparable proportions (Fig. S5). Active C16:0 mono-desaturation was induced in cultures acclimated to low temperature in the four strains, again with greater amplitudes in the subpolar strain MVIR-18-1 and the cold-temperate strain BL107, along with a weak increase in the C14:1 proportion (Fig. 4D, S9, S13).

Double desaturation processes - We used the C16:2 to C16:1 ratio to study the level of double unsaturation of the fatty chains of the different lipids (Fig. 5, S3-S6). Interestingly, double unsaturations occurred exclusively on C16 chains, at the *sn*-1 position of the two galactolipids. The global level of double unsaturation was quite high in the strains adapted to warm environments, WH8102 and A15-62, whereas C16:2 chains were hardly detected in the cold-temperate and subpolar strains BL107 and MVIR-18-1 (Fig. 5). Noteworthy, strain WH8102

responded to low temperature by a large induction of 16:2 at the *sn*-1 of MGDG and, to a lesser extent, DGDG. The capacity for efficient double desaturation activity of strain WH8102 was also observable during the cold shift experiments (Fig. S7).

Metagenomics of lipid-desaturase genes

Previous studies have shown that marine *Synechococcus* temperature ecotypes display different sets of genes encoding lipid-desaturases, including the Δ9-desaturases DesC3 and DesC4 and the Δ12-desaturases DesA2 and DesA3 (Notes S3; Varkey *et al.*, 2016; Pittera *et al.*, 2018). In order to complement the results obtained on strains representative of cold- (I and IV) and warm-adapted (II and III) clades, we used the *Tara* Oceans dataset to study the global distribution and prevalence of the four desaturase genes along natural thermal gradients (Fig. 6).

The prevalence of the *des*C3 gene was close to 1 at all stations, independently of the seawater temperature and ESTU composition (Fig. 6B). This shows that this desaturase gene is present in all *Synechococcus* cells *in situ* in a single copy, just like *pet*B. By contrast, the *desC4* gene was virtually absent from waters warmer than 20°C (Fig. 6C). Below this threshold, the prevalence of this gene increased quasi linearly as seawater temperature decreased, reaching values close to 1 in 13°C waters. This gene was most abundant in populations colonizing waters below 17°C, dominated by *Synechococcus* ESTUs IA and IVA-C (Farrant *et al.*, 2016).

The prevalence of the *des*A2 gene, which encodes a Δ12-desaturase inserting a double unsaturation, showed its maximal value of c.a. 1 for temperatures higher than 20°C (Fig. 6D). Below this temperature, the prevalence progressively decreased down to zero for seawater temperatures lower than 14°C. In this dataset, the *des*A2 gene is mostly present in populations dominated by *Synechococcus* ESTUs IIA and IIIA.

The other Δ12-desaturase, desA3, showed a similar global pattern to the desC4 gene with a marked shift in the relative abundance of this gene between populations dominated by *Synechococcus* ESTUs IA and IVA-C, colonizing waters below 18°C and those dominated by ESTU IIA, thriving in waters above this temperature. In contrast, it is worth noting that in Mediterranean Sea stations dominated by *Synechococcus* ESTU IIIA, the desA3 gene prevalence remained high independently from temperature (Fig. 6E), consistently with the fact that desA3 is

present in the genome of all strains representative of clade III, while it is generally absent from most clade II strains (Pittera et al., 2018).

Discussion

Photosynthesis regulation in cold- and warm-adapted Synechococcus *ecotypes*

Previous studies have shown that adaptation to temperature in marine *Synechococcus* relies on the existence of physiologically specialized lineages that have colonized different thermal environments (Pittera *et al.*, 2014; Varkey *et al.*, 2016). Strains used in the present study have been isolated in water masses with contrasted temperatures, from tropical to subpolar habitats, and belong to the four major *Synechococcus* clades (Table 1). The study of their thermal *preferenda* showed that the two strains isolated from warm environments, *Synechococcus* spp. A15-62 (clade II) and WH8102 (clade III), were able to grow at temperatures higher than 30°C. This result is consistent with previous studies on the Sargasso Sea strains WH8103 (clade III) and WH7803 (clade V; Moore *et al.*, 1995; Pittera *et al.*, 2014, 2018). In contrast, BL107 (clade IV) and MVIR-18-1 (clade I) strains, isolated from temperate and subpolar environments respectively, could not cope with these high temperatures but were able to grow down to 12°C or less (Fig. 1A). These results are in good agreement with previous observations that clades I and IV cells predominate in relatively cold environments, whereas clades II and III preferentially thrive in warmer waters (Zwirglmaier *et al.*, 2008; Sohm *et al.*, 2015; Farrant *et al.*, 2016; Paulsen *et al.*, 2016; Kent *et al.*, 2018). Moreover, it worth noting that these differences in thermal *preferenda* would be likely even more apparent with cultures grown under higher light irradiance, as discussed in previous studies (Pittera *et al.*, 2014, 2018).

All four strains managed to maintain fairly high photosystem II quantum yield over their whole temperature growth range, showing an efficient acclimation of their photosynthetic apparatus to different temperatures (Fig. 1B). Pigment analyses suggest that this ability partly relies upon changes in the relative proportions of major pigments in thylakoid membranes, which differed between strains. *Synechococcus* spp. WH8102 and A15-62 showed a marked increase of the β-carotene to chl *a* ratio in response to high growth temperature, whereas this increase was

moderate in cold-adapted strains (Fig. 1C). Such variations might originate from a change in the photosystem (PS) ratio since these complexes bind the two pigments in fixed but very different proportions. As the β-carotene to chl *a* molar ratio is 0.23 in PSI (Xu & Wang, 2017) and 0.31 in PSII monomers (Umena *et al.*, 2011), our results thus suggest an increase of the PSII to PSI ratio in response to high temperatures. This would lead to decrease the cyclic electron transport around PSI and increase the transthylakoidal pH gradient, then enhancing the ATP production in the cytosol of the warm adapted ecotypes at high growth temperature. In addition, β-carotene and chl *a* molecules have recently been found to be bound to High Light Inducible Proteins (HLIPs) in *Synechocystis* sp. PCC 6803, which are stress-inducible proteins allowing dissipation of excess light (Dolganov *et al.*, 1995; Komenda & Sobotka, 2016). The characterized proteins, whose dissipative activity is temperature-dependent, have a 0.33 (HliD) and 0.5 (HliC) β-carotene to chl *a* ratio (Staleva *et al.*, 2015; Shukla *et al.*, 2018). Even though such proteins have never been biochemically characterized in marine *Synechococcus*, their genomes contain many *hli* genes, which likely encode similar pigmented proteins (Bhaya *et al.*, 2002; Scanlan *et al.*, 2009). Therefore, the regulation of such proteins might also be involved in temperature acclimation in marine *Synechococcus*, especially in the warm-adapted strains WH8102 and A15-62.

In all strains, the zeaxanthin to chl *a* ratio increased in response to low temperature (Fig. 1D). Moreover, this ratio was globally higher in the cold-adapted strains MVIR-18-1 and BL107. Variations of the zeaxanthin to chl *a* ratio likely originated partly from a decrease of the chl *a* cell content, a classical cold-induced response, in order to regulate light utilization in slow growth conditions (Inoue *et al.*, 2001). However, an upregulation of the zeaxanthin synthesis was also most likely involved, as suggested by the increase of the zeaxanthin to β-cryptoxanthin ratio (Fig. S2), the latter pigment being directly converted to zeaxanthin by the β-carotene hydroxylase (CrtR). Even though the localization and function of zeaxanthin have never been formally demonstrated in marine *Synechococcus*, it could have a role in photoprotection by dissipating excess light under low temperature conditions, a process seemingly more prevalent in cold-adapted strains (Fig. 1). On another hand, it is well known that the integration of polar xanthophylls into biological and model membranes strongly affects their properties (for a review see Popova and Andreeva, 2013). If zeaxanthin occurs as a free molecule in marine *Synechococcus* thylakoids, it is expected to decrease the membrane fluidity at low temperature,

as shown in Antarctic bacteria (Jagannadham *et al.*, 2000). Yet, this potentially deleterious increase in membrane rigidity at low temperature seems to be counteracted by modifications of the membrane composition in order to maintain proper membrane fluidity.

Marine Synechococcus thermoregulate the membrane composition differently

Analysis of all molecular species of membrane lipids in four phylogenetically and physiologically distinct strains, as well as comparisons with our previous data on the model strain WH7803 (Pittera *et al.*, 2018), allowed us for the first time to draw a broad picture of the composition of the membranes in marine *Synechococcus*. These five strains exhibit general features that seem to be specific of this group, including notably the variability of the chain bound to the SQDG *sn*-2 position and the relative insensitivity of the composition of PG to temperature (Murata & Wada, 1995; Pittera *et al.*, 2018). Also in sharp contrast to freshwater strains, all five marine *Synechococcus* strains contain very low relative concentrations of C18 chains and are C14-rich. Therefore, while freshwater strains have C18 and C16 at the *sn*-1 and *sn*-2 positions respectively, marine *Synechococcus* lipids preferentially bind C16 and C14 at these positions, respectively. This fatty acid composition implies that marine *Synechococcus* thylakoids are probably thinner and globally more fluid than those of freshwater strains. This is also in good agreement with the much smaller cell volume of these picocyanobacteria compared to their freshwater counterparts. In addition, it is worth noting that C14:0 is usually one of the major fatty acids in samples from surface ocean regions (see e.g. Wakeham and Canuel, 1988; Van Mooy and Fredricks, 2010). Thus, the finding that C14 dominates in all marine *Synechococcus* strains investigated so far further confirms that marine picocyanobacteria are a major source of this lipid in the oceans.

Some strains have however the capacity to modify the C16:C14 ratio, and thus to modulate the membrane thickness. Indeed, our results and a previous study show that, whereas it slightly increased in BL107 (clade IV) and WH8102 (clade III) in response to cold temperature, strains MVIR-18-1 (clade I), A15-62 (clade II) and WH7803 (clade V) were able to significantly decrease the membrane thickness by synthetizing *de novo* shorter lipids, therefore increasing its fluidity (Fig. 2; Pittera *et al.*, 2018). As these strains inhabit very different thermal environments, the capacity to carry out this process does not appear to be related to the thermotype

differentiation. In order to better understand these different responses, future research should investigate the influence of other abiotic parameters, on a larger number of strains.

In response to temperature variations, the *Synechococcus* strains deployed a panel of different desaturation activities. Our result show that the cold-adapted strains MVIR-18-1 (clade I) and BL107 (clade IV) can carry out extensive desaturation of fatty acid mono-desaturation, on both C16 and C14 chains and at both *sn* positions of the three membrane glycolipids (Figs. 3, 4). Noteworthy, the primary Δ9 monounsaturations are expected to have larger membrane fluidifying effects than the secondary Δ12 unsaturations (Hyvonen *et al.*, 1997; Hyvonen & Kovanen, 2005; Ollila *et al.*, 2007). These large Δ9 monodesaturation capacities are thus likely critical for tolerance to low temperature. The warm-adapted strains A15-62 (clade II) and WH8102 (clade III) were overall able to carry out lower monodesaturation activities (Figs. 3, 4). Nevertheless, the tropical A15-62 strain showed stable and relatively high 16:2 content in the galactolipids and WH8102 grown at low temperature (Figs. 5 and S7) induced the highest contents of double unsaturations, whereas these were only detected at trace levels in the cold-adapted strains. Thus, in contrast to cold-adapted strains, strains adapted to warm environments seem to display much higher relative contents of double insaturated fatty acids in their membranes.

Synechococcus *thermotypes use different lipid-desaturase enzymes*

The five strains of marine *Synechococcus* studied to date in the context of membrane lipid thermoacclimation capacities possess different sets of desaturase genes (Pittera *et al.*, 2018; Table 1). The lipidomic analyses showed that all strains were able to induce Δ9-monodesaturations, which is consistent with the presence of *desC3* in all strains. The lipidic profiles of the A15-62 and WH8102 strains (Figs. 3, 4), which only possess DesC3 to synthesize monounsaturated chains, show that this enzyme can incorporate Δ9 double bonds on the three glycolipids, at the two *sn* positions and on both palmitic (C16:0) and myristic (C14:0) chains. Therefore, it appears to be a poorly regiospecific enzyme, responsible for the basal (but essential) monodesaturation capacity of all marine *Synechococcus*. The cold-adapted strains MVIR-18-1 and BL107, which contain an additional Δ9-desaturase gene (Table 1), *desC4*, showed increased monodesaturation capacities. This gene, thought to have derived from a recent gene

duplication event (Pittera *et al.*, 2018), could then provide additional monodesaturation capacity in order to cope with lower temperatures. However, on the lipids of these cold-adapted strains, we could not evidence sites of monodesaturation that would be specific of the DesC4 enzyme. Therefore, our results suggest that the two DesC enzymes in marine *Synechococcus* are rather generalist monodesaturases of the C16 and C14 chains of glycolipids, *i.e.* display a relatively weak regiospecificity. This contrasts with the DesC1 and DesC2 enzymes of freshwater strains, which show differential site specificities (Chintalapati *et al.*, 2006). Future work should aim at studying the possible induction of the *desC4* gene by low temperature, which would provide further evidence of a monodesaturation booster function of the DesC4 enzyme in marine *Synechococcus*.

Double unsaturations were detected mostly in A15-62 and WH8102, which like all other warm-adapted ecotypes sequenced to date, possess a specific Δ12-desaturase, DesA2 (Table 1). In contrast to monounsaturations, the double unsaturations are located specifically on C16 chains at the *sn*-1 of the galactolipids binding a C14:1 chain at the *sn*-2 site, indicating a high level of regiospecificity of DesA enzymes in marine *Synechococcus*. It is worth noting that the WH8102 strain possesses two Δ12-desaturases, DesA3 and DesA2. This likely allows this strain to induce the strong double desaturation activities that were observed in response to low temperature (Fig. 5, Fig. S7H, K). The role of DesA3 in cold-adapted strains remains enigmatic since very few double unsaturations were detected in these strains both in acclimated cultures and temperature shift experiments. It is possible that, in these strains, this enzyme is activated in response to other environmental factors, such as high irradiance.

The lipid-desaturase genes show differential distributions in the Ocean

In order to provide more insights about the physiological strategies used by *Synechococcus* temperature ecotypes to thermoregulate their membranes, we studied the distribution of the four lipid desaturase genes at 33 widespread stations along the *Tara* Oceans transect (Fig. 6A). As expected, the core gene *desC3* displayed a temperature-independent distribution. In contrast, the Δ9-desaturase gene *desC4*, which is specific of cold-adapted strains (Table 1), was found exclusively in waters colder than 20°C, consistent with its hypothesized role of monodesaturation enhancer enabling growth in cold thermal environments.

The *desA2* distribution displayed a mirror pattern with regard to *desC4*, confirming that this Δ12-desaturase is specific of warm environments, dominated by either clade II or clade III *Synechococcus* cells. Like *desC4*, the Δ12-desaturase gene *desA3* was abundant in waters colder than 20°C. This gene was also abundant between 17 and 25°C, but specifically in assemblages dominated by clade III strains, consistent with the presence of this gene in all clade III but no clade II strains sequenced thus far (Table 1). Clade III *Synechococcus* are most abundant in oligotrophic, P-limited areas such as the Mediterranean Sea (Mella-Flores *et al.*, 2011; Farrant *et al.*, 2016), which is subjected to a strong seasonality, being warm in summer (up to 30°C) but cold in winter, with minimal temperatures as low as 13°C in the northwestern basin. Our results thus suggest that the presence of both *desC2* and *desC3* genes confers fitness to clade III strains, which are subjected to much stronger seasonal variability over the year than their (sub)tropical clade II counterparts.

Conclusion and perspectives

Our study shows that marine *Synechococcus* temperature ecotypes can manage, *via* different mechanisms, to regulate their photosynthetic apparatus in order to maintain optimal photosynthetic capacity over most of their respective temperature growth range. We also show that marine *Synechococcus* have evolved different physiological strategies based on the presence of specific lipid desaturase gene sets, allowing them to cope with changes in the fluidity of photosynthetic membrane in different thermal niches. Even though more work such as mutant characterization is necessary, our data allow to propose functions and ecological roles for the four *Synechococcus* desaturases. DesC3 is a constitutive Δ9-desaturase with weak regiospecificity and its activity is probably mostly temperature-independent. *Synechococcus* strains belonging to clades I and IV use an additional enzyme, DesC4, which provide them with enhanced Δ9 monodesaturation capacities and allow to greatly increase the membrane fluidity in cold environments. The occurrence of the *desC4* gene, likely by duplication of its common ancestor with *desC3* (Pittera *et al.*, 2018), has probably been an important event for the colonization of high latitude environments by marine *Synechococcus*. In warm environments, there is little need to perform strong variations of the membrane fluidity and marine *Synechococcus* have seemingly

adopted a different strategy. Clade II strains, which live in warm and stable environments, have globally poor desaturation capacities. However, they constitutively contain membrane lipids with more double unsaturation thanks to DesA2, a Δ12-desaturase specific of warm environments. In warm-temperate environments, where temperature is more variable, clade III strains use the combination of two Δ12-desaturases DesA2 and DesA3. They confer high capacities of double desaturations, which probably help tolerating the low winter temperatures in this niche. The preferential use of double unsaturations, which have less influence on the membrane fluidity than the monounsaturations, likely allows a finer tuning of this physical property in the thermal environments of clade II and III strains than their cold-adapted counterparts. An alternative hypothesis is that Δ12-desaturases might be most efficient at high temperature, while Δ9-desaturases were selected in colder environments during the evolution of marine *Synechococcus*. In conclusion, this study strongly suggests that the capacity to greatly modulate membrane fluidity has been critical for the colonization of different thermal niches by marine *Synechococcus*, leading to the differentiation in physiologically distinct temperature ecotypes. It furthermore shows that lipid-desaturase genes are interesting markers for monitoring the dynamics of ocean microbial communities in the global change context.

Acknowledgements

This work was funded by the French programs EC2CO-Microbien (METALIC), ANR CINNAMON (ANR-17-CE2-0014-01) and EMBRC France (INFRA-2010-2.2.5). Solène Breton and Ulysse Guyet were supported by the Région Bretagne and the French Ministry of Higher Education and Research. Juliette Jouhet and Eric Maréchal are supported by the French National Research Agency (ANR-10-LABEX-04 GRAL Labex, Grenoble Alliance for Integrated Structural Cell Biology; ANR-11-BTBR-0008 Océanomics; ANR-15-IDEX-02 GlycoAlps Cross DisciplinaryProject). We are grateful to the Roscoff Culture Collection for maintaining the *Synechococcus* strain used in this study. We thank the ABIMS Platform (Station Biologique de Roscoff) for their help in the metagenomics data computing. We also thank the support and commitment of the *Tara* Oceans coordinators and consortium, Agnès B. and E. Bourgois, the Veolia Environment Foundation, Region Bretagne, Lorient Agglomeration, World Courier, Illumina, the EDF Foundation, FRB, the

Prince Albert II de Monaco Foundation, and the *Tara* schooner and its captains and crew. *Tara* Oceans would not exist without continuous support from 23 institutes (oceans.taraexpeditions.org). We certify that there is no conflict of interest associated with this manuscript.

Author contribution

CS, LG and FP designed the research. SB, JJ, UG, VG, JP, DD, FP, HD, MR, EM, NAN, LG, CS contributed to the performance of this work and the analysis of the data. CS, LG, FP, SB, NN, JJ, EM, UG and DD worked on the writing of the manuscript.

List of the tables and legends

Table 1: Characteristics of the four *Synechococcus* strains used in this study. Taxonomic assignment at the clade level and desaturase gene content are derived from Farrant *et al.* (2016) and Pittera *et al.* (2018), respectively. The average seawater temperature is the annual mean temperature at the isolation site of the strain over the 2000-2010 period, as derived from the NASA Sea Surface Temperature data (https://oceandata.sci.gsfc.nasa.g). The modelled values of thermal limits of growth were calculated using the phytoplankton growth model defined by Boatman *et al.* (2017). Presence of a desaturase gene in a strain is indicated by grey color.

Figure 1: Variations of growth rates (**A**), photosystem II quantum yield (F_V/F_M; **B**) and membrane pigment mass ratios (**C**, **D**) in *Synechococcus* sp. MVIR-18-1 (blue circles), BL107 (green diamonds), WH8102 (orange triangles) and A15-62 (red squares), acclimated to a range of temperatures spanning from 10°C to 30°C. Zea: zeaxanthin; Chl *a*: chlorophyll *a*; β-car: β-carotene. Measurements are average of four replicates with error bars ± SD.

Figure 2: Variations of the C14 to C16 molar ratio, related to the average length of the fatty acid bound to the *sn*-1 position of the monogalactosyldiacylglycerol (MGDG, **A**) and the digalactosyldiacylglycerol (DGDG, **B**) for the four marine *Synechococcus* strains: MVIR-18-1 (blue circles), BL107 (green diamonds), WH8102 (orange triangles) and A15-62 (red squares), acclimated to a range of temperatures spanning from 10°C to 30°C. Measurements are average of three to four replicates with error bars ± SD.

Figure 3: Variations of the mono-desaturation level, expressed as the C16:1 to C16:0 (left) and C14:1 to C14:0 (right) molar ratios, of the fatty acid bound to the *sn*-1 position of the monogalactosyldiacylglycerol (MGDG, **A** and **B**), digalactosyldiacylglycerol (DGDG, **C** and **D**) and sulfoquinovosyldiacylglycerol (SQDG, **E** and **F**) for the four marine *Synechococcus* strains: MVIR-18-1 (blue circles), BL107 (green diamonds), WH8102 (orange triangles) and A15-62 (red squares), acclimated to a range of temperatures spanning from 10°C to 30°C. Measurements are average of three to four replicates with error bars ± SD.

Figure 4: Variations of the mono-desaturation level, expressed as the C16:1 to C16:0 (left) and C14:1 to C14:0 (right) molar ratios, of the C14 fatty acid bound to the *sn*-2 position of the

monogalactosyldiacylglycerol (MGDG, **A**) and the digalactosyldiacylglycerol (DGDG, **B**) and sulfoquinovosyldiacylglycerol (SQDG, **C** and **D**) for the four marine *Synechococcus* strains acclimated MVIR-18-1 (blue circles), BL107 (green diamonds), WH8102 (orange triangles), and A15-62 (red squares), acclimated to a range of temperatures spanning from 10°C to 30°C Measurements are average of three to four replicates with error bars ± SD.

Figure 5: Variations of the double-desaturation level, expressed as C16:2 to C16:1 molar ratios, of the fatty acid bound to the *sn*-1 position of the monogalactosyldiacylglycerol (MGDG, **A**), digalactosyldiacylglycerol (DGDG, **B**), for the four marine *Synechococcus* strains acclimated MVIR-18-1 (blue circles), BL107 (green diamonds), WH8102 (orange triangles), and A15-62 (red squares) acclimated to a range of temperatures spanning from 10°C to 30°C. Measurements are average of three to four replicates with error bars ± SD.

Figure 6: Localization of the stations of the *Tara* Oceans expedition used in this study (**A**), and prevalence of the Δ9 lipid-desaturase genes *desC3* (**B**), *desC4* (**C**) and the Δ12 lipid-desaturase genes *desA2* (**D**) and *desA3* (**E**), as a function of seawater temperature at these stations. This was determined using metagenomic data from the *Tara* Oceans expedition for stations dominated by major Ecologically Significant Taxonomic Units (ESTUs) *sensu* Farrant *et al.* (2016) within *Synechococcus* clades I to IV. At each station, the relative abundance of each desaturase gene was normalized by the relative abundance of the core, single-copy gene *petB* The LOESS regression model was used as curve fitting method with a span α = 0.8 using the ggplot2 R package (https://cran.r-project.org/web/packages/ggplot2/index.html). The grey shading areas correspond to the 95% confidence interval.

References

Altschul SF, Gish W, Miller W, Myers EW, Lipman DJ. **1990**. Basic Local Alignment Search Tool. *Journal of Molecular Biology* **215**: 403–410.

Bernard O, Rémond B. **2012**. Validation of a simple model accounting for light and temperature effect on microalgal growth. *Bioresource Technology* **123**: 520–527.

Bhaya D, Dufresne A, Vaulot D, Grossman A. **2002**. Analysis of the hli gene family in marine and freshwater cyanobacteria. *FEMS Microbiology Letters* **215**: 209–219.

Bligh E, Dyer W. **1959**. A rapid method of total lipid extraction and purification. *Canadian Journal of Biochemistry and Physiology* **37**: 911–917.

Boatman TG, Lawson T, Geider RJ. **2017**. A key marine diazotroph in a changing ocean: The interacting effects of temperature, $C0_2$ and light on the growth of *Trichodesmium erythraeum* IMS101. *PLoS ONE* **12**: 1–20.

Campbell DA, Hurry V, Clarke AK, Gustafsson P, Oquist G. **1998**. Chlorophyll fluorescence analysis of cyanobacterial photosynthesis and acclimation. *Microbiology and molecular biology reviews* **62**: 667–683.

Chi X, Yang Q, Zhao F, Qin S, Yang Y, Shen J, Lin H. **2008**. Comparative analysis of fatty acid desaturases in cyanobacterial genomes. *Comparative and Functional Genomics* **2008**: 1–25.

Chintalapati S, Prakash JSS, Gupta P, Ohtani S, Suzuki I, Sakamoto T, Murata N, Shivaji S. **2006**. A novel Delta9 acyl-lipid desaturase, DesC2, from cyanobacteria acts on fatty acids esterified to the sn-2 position of glycerolipids. *The Biochemical journal* **398**: 207–14.

Coleman ML, Chisholm SW. **2007**. Code and context: *Prochlorococcus* as a model for cross-scale biology. *Trends in Microbiology* **15**: 398–407.

Dolganov NA, Bhaya D, Grossman AR. **1995**. Cyanobacterial protein with similarity to the chlorophyll a/b binding proteins of higher plants: evolution and regulation. *Proceedings of the National Academy of Sciences of the United States of America* **92**: 636–640.

Farrant GK, Doré H, Cornejo-Castillo FM, Partensky F, Ratin M, Ostrowski M, Pitt FD, Wincker P, Scanlan DJ, Iudicone D, *et al.* 2016. Delineating ecologically significant taxonomic units from global patterns of marine picocyanobacteria. *Proceedings of the National Academy of Sciences* **113**: E3365–E3374.

Flombaum P, Gallegos JL, Gordillo RA, Rincon J, Zabala LL, Jiao N, Karl DM, Li WKW, Lomas MW,

Veneziano D, *et al.* 2013. Present and future global distributions of the marine Cyanobacteria *Prochlorococcus* and *Synechococcus*. *Proceedings of the National Academy of Sciences* **110**: 9824–9829.

Herdman M, Castenholz RW, Waterbury JB, Rippka R. **2001**. Form-genus XIII. *Synechococcus*. In: Bergey's Manual of Systematic Bacteriology. 508–512.

Huang S, Wilhelm SW, Harvey HR, Taylor K, Jiao N, Chen F. **2012**. Novel lineages of *Prochlorococcus* and *Synechococcus* in the global oceans. *The ISME journal* **6**: 285–97.

Hyvonen MT, Ala-korpela M, Vaara J, Rantala TT, Jokisaari J. **1997**. Inequivalence of single CHa and CHb methylene bonds in the interior of a diunsaturated lipid bilayer from a molecular dynamics simulation. *Chemical Physics Letters* **268**: 55–60.

Hyvonen MT, Kovanen PT. **2005**. Molecular dynamics simulations of unsaturated lipid bilayers: effects of varying the numbers of double bonds. *European Biophysics Journal* **34**: 294–305.

Inoue N, Taira Y, Emi T, Yamane Y, Kashino Y, Koike H, Satoh K. **2001**. Acclimation to the growth temperature and the high-temperature effects on photosystem II and plasma membranes in a mesophilic cyanobacterium, *Synechocystis* sp. PCC 6803. *Plant & cell physiology* **42**: 1140–1148.

Itoh S, Kozuki T, Nishida K, Fukushima Y, Yamakawa H, Domonkos I, Laczkó-Dobos H, Kis M, Ughy B, Gombos Z. **2012**. Two functional sites of phosphatidylglycerol for regulation of reaction of plastoquinone QBin photosystem II. *Biochimica et Biophysica Acta - Bioenergetics* **1817**: 287–297.

Jagannadham M V., Chattopadhyay MK, Subbalakshmi C, Vairamani M, Narayanan K, Rao CM, Shivaji S. **2000**. Carotenoids of an Antarctic psychrotolerant bacterium, *Sphingobacterium antarcticus*, and a mesophilic bacterium, *Sphingobacterium multivorum*. *Archives of Microbiology* **173**: 418–424.

Johnson ZI, Zinser ER, Coe A, Mcnulty NP, Malcolm ES, Chisholm SW, Woodward EMS, Chisholm SW. **2006**. Partitioning Among *Prochlorococcus* Ecotypes Along Environmental Gradients. *Science* **311**: 1737–1740.

Jouhet J, Lupette J, Clerc O, Magneschi L, Bedhomme M, Collin S, Roy S, Maréchal E, Rébeillé F. **2017**. LC-MS/MS versus TLC plus GC methods: Consistency of glycerolipid and fatty acid profiles in microalgae and higher plant cells and effect of a nitrogen starvation. *PLoS ONE* **12**: 1–21.

Kana TM, Glibert PM. **1987**. Effect of irradiances up to 2000 µE m−2 s−1 on marine *Synechococcus* WH7803—I. Growth, pigmentation, and cell composition. *Deep Sea Research Part A.* **34**: 479–495.

Kent AG, Baer SE, Mouginot C, Huang JS, Lomas MW, Martiny AC. **2018**. Parallel phylogeography of *Prochlorococcus* and *Synechococcus*. *ISME Journal* **13**: 430–441.

Komenda J, Sobotka R. **2016**. Cyanobacterial high-light-inducible proteins — Protectors of chlorophyll – protein synthesis and assembly. *Biochimica et biophysica acta - Bioenergetics* **1857**: 288–295.

Los DA, Murata N. **1998**. Structure and expression of fatty acid desaturases. *Biochimica et biophysica acta* **1394**: 3–15.

Mackey KRM, Paytan A, Caldeira K, Grossman AR, Moran D, McIlvin M, Saito MA. **2013**. Effect of temperature on photosynthesis and growth in marine *Synechococcus* spp. *Plant physiology* **163**: 815–29.

Magoč T, Salzberg SL. **2011**. FLASH: Fast length adjustment of short reads to improve genome assemblies. *Bioinformatics* **27**: 2957–2963.

Marie D, Partensky F, Vaulot D, Brussaard C. **2001**. Enumeration of Phytoplankton, Bacteria, and Viruses in Marine Samples. In: Current Protocols in Cytometry. Chapter 11 pp 1-15.

Mazard S, Ostrowski M, Partensky F, Scanlan DJ. **2012**. Multi-locus sequence analysis, taxonomic resolution and biogeography of marine *Synechococcus*. *Environmental Microbiology* **14**: 372–386.

Mella-Flores D, Mazard S, Humily F, Partensky F, Mahé F, Bariat L, Courties C, Marie D, Ras J, Mauriac R, *et al.* 2011. Is the distribution of *Prochlorococcus* and *Synechococcus* ecotypes in the Mediterranean Sea affected by global warming? *Biogeosciences* **8**: 2785–2804.

Merritt M V, Rosenstein SP, Loh C, Hsui-sui Chou R, Allen MM. **1991**. A comparison of the major lipid classes and fatty acid composition of marine unicellular cyanobacteria with freshwater species. *Archives of Microbiology* **155**: 107–113.

Mikami K, Murata N. **2003**. Membrane fluidity and the perception of environmental signals in cyanobacteria and plants. *Progress in Lipid Research* **42**: 527–543.

Mizusawa N, Wada H. **2012**. The role of lipids in photosystem II. *Biochimica et Biophysica Acta - Bioenergetics* **1817**: 194–208.

Moore LR, Coe A, Zinser ER, Saito M a., Sullivan MB, Lindell D, Frois-Moniz K, Waterbury J, Chisholm SW. **2007**. Culturing the marine cyanobacterium *Prochlorococcus*. *Limnology and Oceanography: Methods* **5**: 353–362.

Moore L, Goericke R, Chisholm S. **1995**. Comparative physiology of *Synechococcus* and *Prochlorococcus*:

influence of light and temperature on growth, pigments, fluorescence and absorptive properties. *Marine Ecology Progress Series* **116**: 259–275.

Van Mooy BAS, Fredricks HF. **2010**. Bacterial and eukaryotic intact polar lipids in the eastern subtropical South Pacific: Water-column distribution, planktonic sources, and fatty acid composition. *Geochimica et Cosmochimica Acta* **74**: 6499–6516.

Van Mooy B a S, Fredricks HF, Pedler BE, Dyhrman ST, Karl DM, Koblízek M, Lomas MW, Mincer TJ, Moore LR, Moutin T, *et al.* 2009. Phytoplankton in the ocean use non-phosphorus lipids in response to phosphorus scarcity. *Nature* **458**: 69–72.

Murata N, Wada H. **1995**. Acyl-lipid desaturases and their importance in the tolerance and acclimatization to cold of cyanobacteria. *Biochemical Journal* **308**: 1–8.

Ogawa T, Misumi M, Sonoike K. **2017**. Estimation of photosynthesis in cyanobacteria by pulse-amplitude modulation chlorophyll fluorescence: problems and solutions. *Photosynthesis Research* **133**:63-73.

Ollila S, Hyvonen MT, Vattulainen I. **2007**. Polyunsaturation in Lipid Membranes : Dynamic Properties and Lateral Pressure Profiles. *Journal of Physical Chemistry B* **111**: 3139–3150.

Paulsen ML, Doré H, Garczarek L, Seuthe L, Müller O, Sandaa R, Bratbak G, Larsen A. **2016**. *Synechococcus* in the Atlantic Gateway to the Arctic Ocean. *Frontiers in Marine Science* **3**: 1–14.

Pittera J, Humily F, Thorel M, Grulois D, Garczarek L, Six C. **2014**. Connecting thermal physiology and latitudinal niche partitioning in marine *Synechococcus*. *The ISME journal* **8**(6):1221-36.

Pittera J, Jouhet J, Breton S, Garczarek L, Partensky F, Maréchal É, Nguyen NA, Doré H, Ratin M, Pitt FD, *et al.* 2018. Thermoacclimation and genome adaptation of the membrane lipidome in marine *Synechococcus*. *Environmental Microbiology* **20**: 612–631.

Pittera J, Partensky F, Six C. **2016**. Adaptive thermostability of light-harvesting complexes in marine picocyanobacteria. *The ISME Journal* **11**: 1–13.

Popova A V., Andreeva AS. **2013**. *Carotenoid-Lipid Interactions*. Copyright © 2013 Elsevier Inc. All rights reserved.

Rippka R, Coursin T, Hess W, Lichtlé C, Canlan DJ, Palinska KA, Iteman I, Partensky F, Houmard J, Herdman M. **2000**. *Prochlorococcus marinus* Chisholm et al. 1992 subsp. *pastoris* subsp. nov. strain PCC 9511, the first axenic chlorophyll a2/b2-containing cyanobacterium (Oxyphotobacteria). *International*

Journal of Systematic and Evolutionary Microbiology **50**: 1833–1847.

Scanlan DJ, Ostrowski M, Mazard S, Dufresne A, Garczarek L, Hess WR, Post AF, Hagemann M, Paulsen I, Partensky F. **2009**. Ecological genomics of marine picocyanobacteria. *Microbiology and molecular biology reviews : MMBR* **73**: 249–299.

Shukla MK, Llansola MJ, Martin P, Andrew T, Bruno AP, Sobotka R. **2018**. Binding of pigments to the cyanobacterial high-light-inducible protein HliC. *Photosynthesis Research* **137**: 29–39.

Sohm JA, Ahlgren NA, Thomson ZJ, Williams C, Moffett JW, Saito MA, Webb EA, Rocap G. **2015**. Co-occurring *Synechococcus* ecotypes occupy four major oceanic regimes defined by temperature, macronutrients and iron. *The ISME Journal* **10**: 1–13.

Staleva H, Komenda J, Shukla MK, Kan R, Sobotka R. **2015**. Cyanobacterial ancestor of plant antenna proteins. *Nat. Chem. Biol.* **11**: 287–291.

Sunagawa S, Coelho LP, Chaffron S, Kultima JR, Labadie K, Salazar G, Djahanschiri B, Zeller G, Mende DR, Alberti A, *et al.* 2015. Ocean plankton. Structure and function of the global ocean microbiome. *Science* **348** (6237):1261359.

Umena Y, Kawakami K, Shen J, Kamiya N. **2011**. Crystal structure of oxygen-evolving photosystem II at a resolution of 1.9 Å. *Nature* **473**: 55–60.

Varkey D, Mazard S, Ostrowski M, Tetu SG, Haynes P, Paulsen IT. **2016**. Effects of low temperature on tropical and temperate isolates of marine *Synechococcus*. *The ISME Journal* **10**: 1252–1263.

Wakeham SG, Canuel EA. **1988**. Organic geochemistry of particulate matter in the eastern tropical North Pacific Ocean: Implications for particle dynamics. *Journal of Marine Research* **46**: 183–213.

Xu W, Wang Y. **2017**. Function and Structure of Cyanobacterial Photosystem I. In: Hou H., Najafpour M., Moore G., Allakhverdiev S. (eds) Photosynthesis: Structures, Mechanisms, and Applications. Springer, Cham, Germany. Chapter 7 pp 111-168

Zwirglmaier K, Jardillier L, Ostrowski M, Mazard S, Garczarek L, Vaulot D, Not F, Massana R, Ulloa O, Scanlan DJ. **2008**. Global phylogeography of marine *Synechococcus* and *Prochlorococcus* reveals a distinct partitioning of lineages among oceanic biomes. *Environmental Microbiology* **10**: 147–161.

Supplementary information

Dataset S1: Desaturase sequences of marine *Synechococcus*/*Cyanobium* used to recruit desaturase reads from Tara Oceans metagenomes.

Dataset S2: Desaturase sequences of *Prochlorococcus* used outgroups to exclude non *Synechococcus*/*Cyanobium* fatty acid desaturase reads recruited from Tara Oceans metagenomes.

Dataset S3: Prokaryotic genomes used as outgroups to exclude non *Synechococcus*/*Cyanobium* desaturase reads recruited from Tara Oceans metagenomes.

Dataset S4: Desaturase sequences used as outgroups to exclude non *Synechococcus*/*Cyanobium* desaturase reads recruited from Tara Oceans metagenomes.

Notes S1: Growth rate modelling and pigment analyses

Notes S2: Membrane lipidomics.

Notes S3: Fatty acid desaturase Metagenomics

Table S1: Parameters calculated with the BR model.

Table S2: Parameters calculated with the Boatman model.

Table S3: Variations of the acyl chains esterified on the MGDG, DGDG, SQDG and PG of *Synechococcus* sp. MVIR-18-1 grown at different temperatures.

Table S4: Variations of the acyl chains esterified on the MGDG, DGDG, SQDG and PG of *Synechococcus* sp. BL107 grown at different temperatures.

Table S5: Variations of the acyl chains esterified on the MGDG, DGDG, SQDG and PG of *Synechococcus* sp. WH8102 grown at different temperatures.

Table S6: Variations of the acyl chains esterified on the MGDG, DGDG, SQDG and PG of *Synechococcus* sp. A15-62 grown at different temperatures.

Figure S1: Growth rate vs. temperature modelled curves with the BR and Boatman models.

Figure S2: Variations of the zeaxanthin to β-cryptoxanthin mass ratio function of growth temperature.

Figure S3: Variations in acyl chains esterified on the MGDG for the four *Synechococcus* strains grown at different temperatures.

Figure S4: Variations in acyl chains esterified on the DGDG for the four *Synechococcus* strains grown at different temperatures.

Figure S5: Variations in acyl chains esterified on the SQDG for the four *Synechococcus* strains grown at different temperatures.

Figure S6: Variations in acyl chains esterified on the PG for the four *Synechococcus* strains grown at different temperatures.

Figure S7: Variations in acyl chains esterified on the MGDG for the four *Synechococcus* strains in response to a temperature shift from 22°C to 13°C.

Figure S8: Variations in acyl chains esterified on the DGDG for the four *Synechococcus* strains in response to a temperature shift from 22°C to 13°C.

Figure S9: Variations in acyl chains esterified on the SQDG for the four *Synechococcus* strains in response to a temperature shift from 22°C to 13°C.

Figure S10: Variations in acyl chains esterified on the PG for the four *Synechococcus* strains grown in response to a temperature shift from 22°C to 13°C.

Figure S11: Variations in the acyl chains esterified on the MGDG for the four *Synechococcus* strains in response to a temperature shift from 22°C to 30°C.

Figure S12: Variations in the acyl chains esterified on the DGDG for the four *Synechococcus* strains in response to a temperature shift from 22°C to 30°C.

Figure S13: Variations in the acyl chains esterified on the SQDG for the four *Synechococcus* strains in response to a temperature shift from 22°C to 30°C.

Figure S14: Variations in the acyl chains esterified on the PG for the four *Synechococcus* strains in response to a temperature shift from 22°C to 30°C.

Breton *et al.*, Table 1

Strain name	RCC #	Clade	Isolation site	Coordinates	Average seawater temperature (°C)	T_{MIN} (°C)	T_{MAX} (°C)	Lipid-desaturase gene content			
								Δ9-desaturase		Δ12-desaturase	
								*des*C3	*des*C4	*des*A2	*des*A3
MVIR-18-1	2385	I	North Sea	+61°0', +1°59'	10.4 ± 0.3	1.0	28.8				
BL107	515	IV	Mediterranean Sea	+43°43', +3°33'	17.9 ± 0.3	10.37	28.4				
A15-62	2374	II	Offshore Mauritania	+17°37', -20°27'	23.7 ± 0.4	9.0	30.8				
WH8102	539	III	Caribbean Sea	+22°29', -65°3'	27.1 ± 0.1	13.9	32.2				

Figure 1

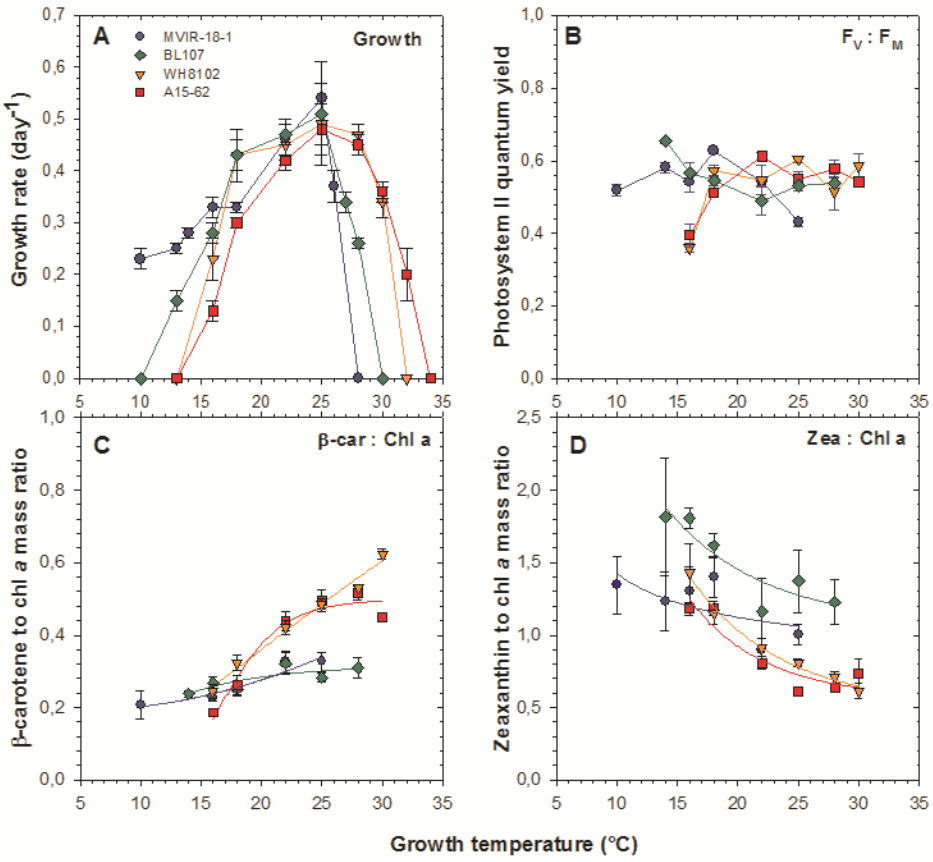

nph_16239_f1.tif

Figure 2

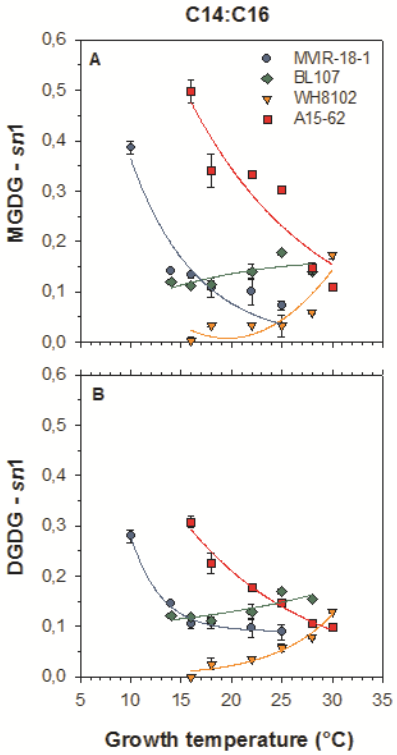

nph_16239_f2.tif

Figure 3

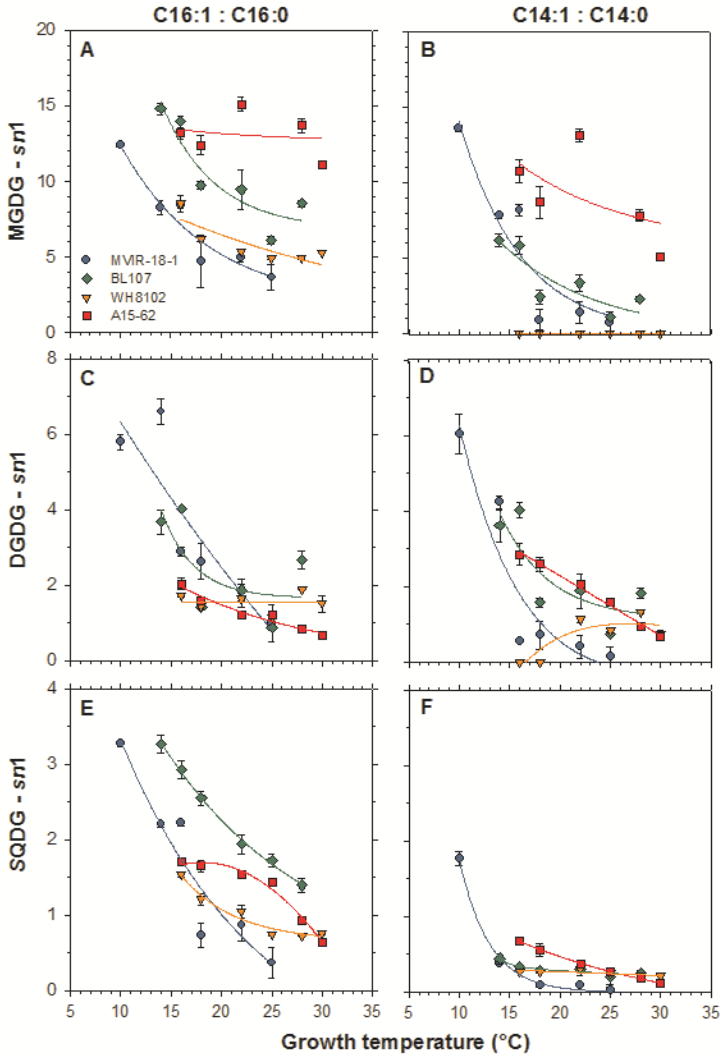

nph_16239_f3.tif

Figure 4

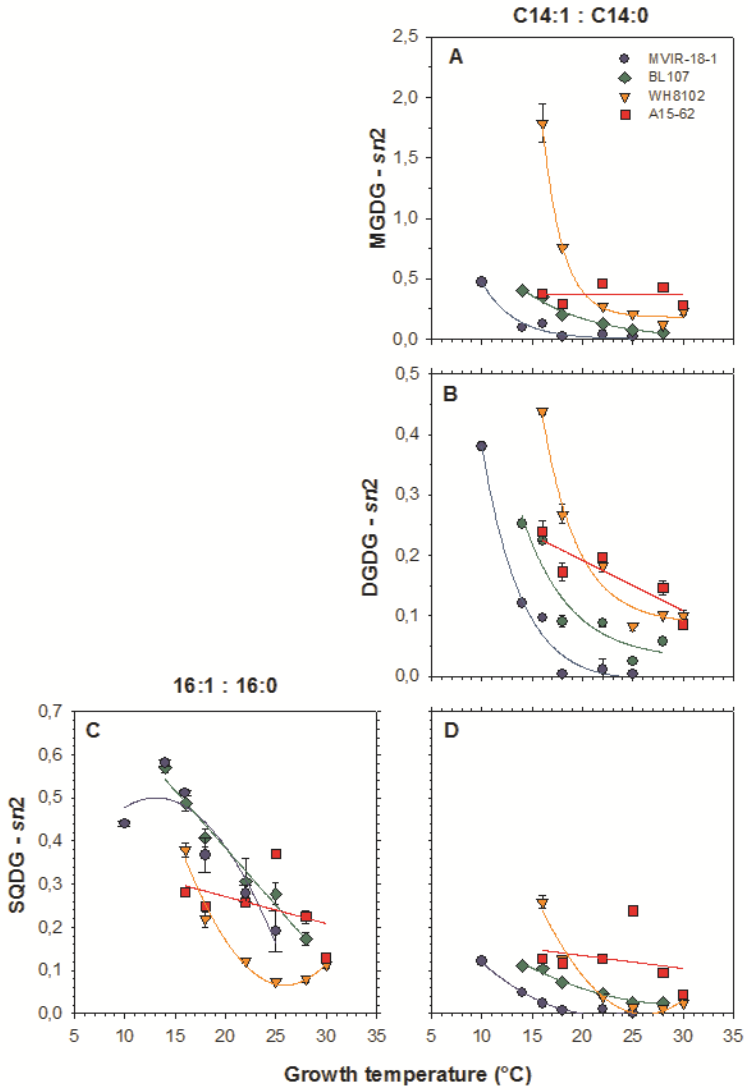

nph_16239_f4.tif

Figure 5

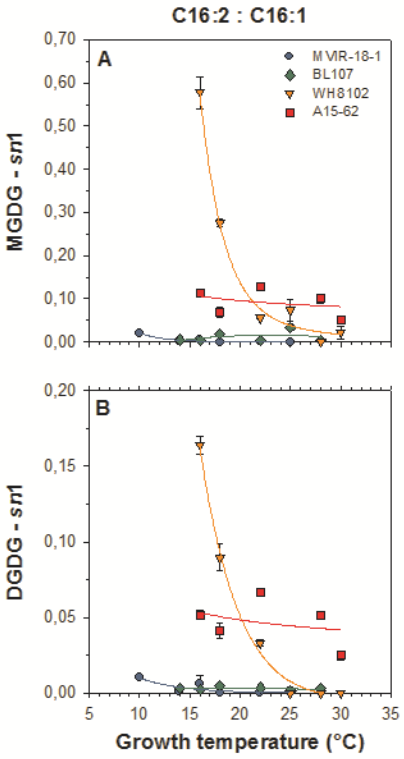

nph_16239_f5.tif

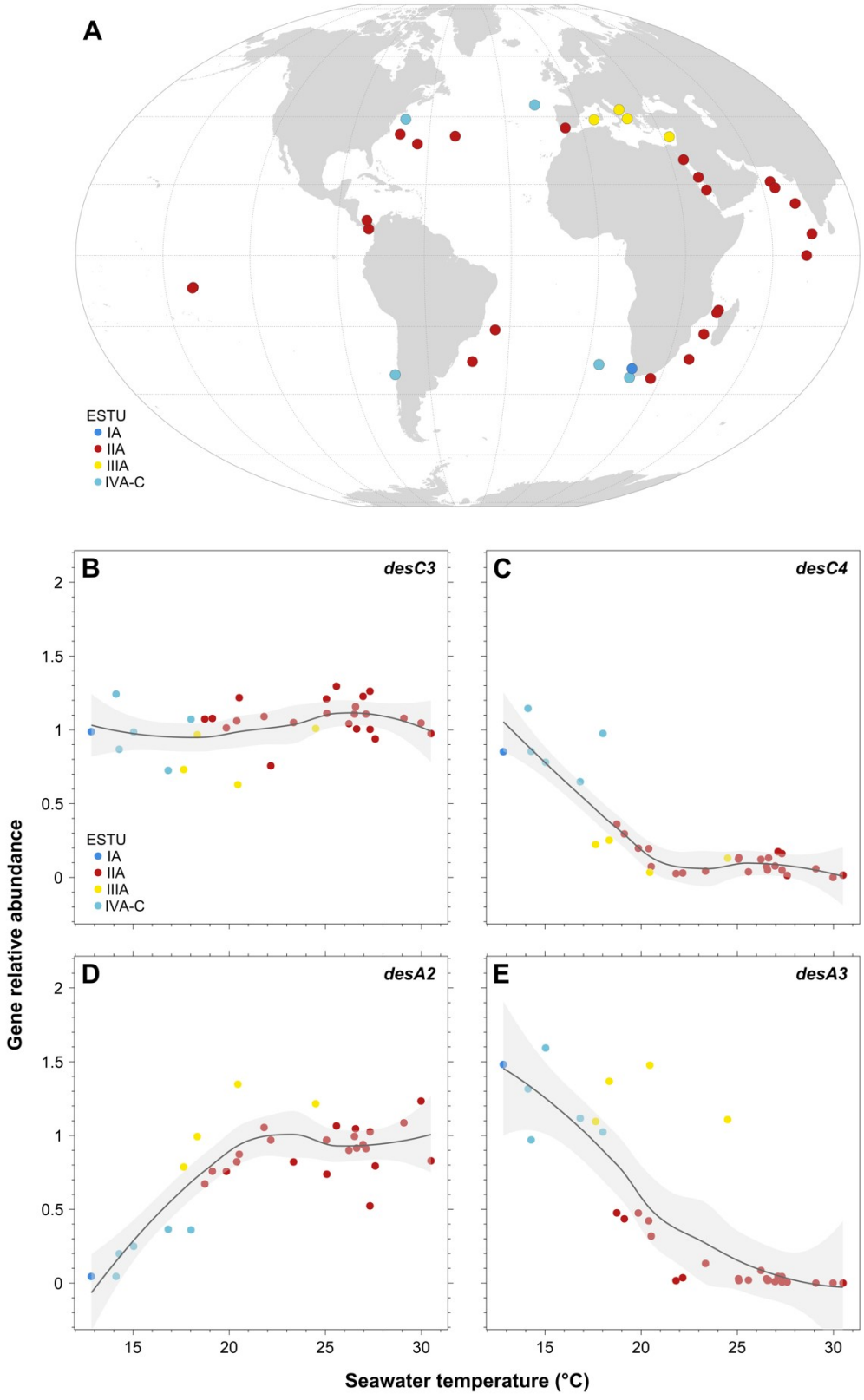

nph_16239_f6.jpg